

## Spatial variability study of rainfall in Cartagena de Indias, Colombia

Javier A. Mouthon-Bello, Edgar Quiñones-Bolaños , Jairo E. Ortiz-Corrales ,  
Natalia Mouthon-Barraza, Maria D.J. Hernández-Fuentes, Andrea C. Caraballo-Meza

Universidad de Cartagena, Faculty of Engineering, Department of Civil Engineering,  
Consulate Ave 30, No. 48-152, 130014, Cartagena de Indias, Colombia

RECEIVED 12.06.2021

ACCEPTED 06.12.2021

AVAILABLE ONLINE 31.12.2022

**Abstract:** Precipitation is a component of the hydrological cycle, knowing its spatial distribution is vital for the management of hydrographic basins, the territory and the development of fundamental activities for society. That is why the present study shows the spatial variability of rainfall in Cartagena de Indias city with a network of rain gauges, made up of nine pieces of equipment, separated from each other by 0.9–27 km. After a year of recording (2019), using historical series of data, it was found that the maximum rainfall occurs in the trimester between September and November, with interpolated maps made by the Ordinary Kriging (OK) method it was found that the maximum rainfall is focused on the north, centre and west of the territory, instead, the maximum intensities are presented in the centre and west, the minimums for both variables are presented to the east and south. The 70 and 90% of the rain events have a duration of less than 30 min and 1 h, respectively. Three-parameter exponential function was fitted to the paired correlation distances, and presented correlations lower than 0.8, 0.5 and 0.2 from distances of 1, 3 and 7 km, respectively, in 30 min rain integration. It was also found that with a pluviometric network conformed by at least six pieces of equipment and separated by a 5 km distance from each other in the urban area, a correlation of 0.5 and compliance with the WMO recommendations would be obtained.

**Keywords:** coastal city, rainfall duration, rainfall intensity, spatial correlation, spatial variability

### INTRODUCTION

Knowing the spatial and temporal variations in precipitation is of great importance for the planning of the territory, classification of land use and development activities such as agriculture [PRIYAN 2015], production of electrical energy, and prevention of natural disasters among other activities that can be considered fundamental for the well-being of humanity [ALFONSO, SCHNABEL 2017]. That is why at national and international levels studies have been carried out in different regions such as Manizales (Colombia) [CORTÉS 2010], Algeria [MERNIZ *et al.* 2019], North Pacific region of Mexico [GARCÍA, CRUZ 2009], Delmarva Peninsula (USA) [TOKAY *et al.* 2014], India [DEY, MUJUMDAR 2019; WARWADE *et al.* 2018] and Greece [MARKONIS *et al.* 2017], where the importance and implications of studying and knowing the variability of rainfall have been pointed out.

To study the spatial variability of rainfall, there is a wide variety of literature and different methodologies used to understand or establish a distribution pattern, authors such as GARRIDO-AREVALO *et al.* [2020], with historical records, have applied concepts from information entropy and artificial neural networks (ANNs) model for assessment of the rainfall station distribution. In that study, meteorological stations were classified for the first time using two-dimensional self-organising maps, raising three scenarios by adjusting the number of neurons in the output layer, then evaluated the performance of the ANNs by applying concepts of information entropy. The methods were tested by experimental datasets, where both the number of groups and their members were previously known. MITRA *et al.* [2018] studied the variation of rainfall during the monsoon season, constructing a Markov random field (MRF) model.

TOKAY *et al.* [2014] and TOKAY and ÖZTÜRK [2012] used a three-parameter stretched exponential model to determine the inter-gauge correlations, establishing a relationship between correlation and distance. For this, 5-year rainfall data were analysed, grouping them by different seasons of the year and periods of event duration. The results were tested by the root-mean-square error (RMSE), which shows the goodness of the fit.

ALFONSO and SCHNABEL [2017] studied the spatial variability of 7 years of rainfall record, comparing the average precipitation methods of the arithmetic mean and the Thiessen polygon, for annual, monthly, daily and seasonal scales, applying the concepts of standard deviation and coefficient of variation between rain gauges. However, the isohyets method was rejected because the study area did not present strong topography contrasts.

Although in many pieces of research the equipment network is already installed or belongs to national institutes, so it is impossible to relocate them, there are equipment location methodologies to select the optimal distribution. GYASI-AGYEI [2020] identified the optimum rain gauge network density, using scaling laws and bias-corrected 1 km × 1 km grid radar rainfall records. Other authors such as ADHIKARY *et al.* [2015] studied the optimal positioning of additional stations as well as optimal relocating of existing redundant ones, reducing the kriging error as an indicator for optimal spatial positioning. The previous methods require prior information which is a disadvantage for a network that will be newly installed, so it is feasible and common to initially use the density per station recommended by the WMO, which then can be optimised by complementing with new pieces of equipment or relocating of the existing ones.

Currently, the city has only one rainfall station that has a historical series of information of more than 30 years, it is located at the Rafael Núñez International Airport. Therefore, there are no other stations that allow a comparison of rainfall at different points of the urban perimeter. In addition, in the absence of studies concerning the spatial variability of rain, it is common to assume that rain occurs uniformly throughout the urban perimeter and in neighbouring areas, which causes solutions to the problems generated by climate change to be incorrectly addressed, with repercussions in the physical-natural, physical-spatial and even socio-economic fields. On the other hand, having a historical record of this natural phenomenon would help in the realisation of plans both for the use of this resource and to prevent landslides, floods, and other natural disasters that may occur within the urban area.

Cartagena de Indias is one of the most important cities in the Colombian Caribbean that suffers from the consequences of climate change and the intensity of extreme phenomena [IPCC 1997]. By 2040 flooding is projected to affect 201108 people as a result of extreme precipitation events [INVEMAR ... 2012], which have intensified to almost 50% more rainfall than the upper range of the normal variation of the wettest month [INVEMAR ... 2014].

The importance of this work lies in the fact that studies have never been carried out to find out the spatial variability of precipitation in the city, its knowledge would contribute to the correct decision-making, in the economic fields, the social and environmental aspects of planning, since all these must contain a significant climatic component that will provide solutions to the requirement of new parameters for the design of protection, control and evacuation work, as well as to the requirement of

clear policies for the occupation and protection of the territory; all these approaches are obeying the current climate conditions. The contribution of this material would also serve to promote the increase of the number of meteorological stations that include rainfall collection in the network of national institutions, as well as promote similar research and methodological guidance for places near Ecuador, the Caribbean or any other place that is of interest to investigate. Thus, the following questions arise.

1. Is there any spatial variation of rainfall in the urban basins of Cartagena de Indias city?
2. How many rainfall stations are required in a tropical coastal zone to counteract the effect generated by the spatial variability of rainfall?

## MATERIAL AND METHODS

### STUDY AREA

Cartagena de Indias city is located in Colombia in the north of the department of Bolívar on the shore of the Caribbean Sea. It is located at 10°25'30" N and 75°32'25" W with respect to the Greenwich meridian, in a typical, rugged and irregular coastal area, formed by geological processes related to the sea [CIOH 2011], as seen in Figure 1. Cartagena has an area of 609.1 km<sup>2</sup>, of which the urban area makes about 80 km<sup>2</sup> (12.8%) [Alcaldia ... 2001; EPA Cartagena 2019]. Its maximum, average and minimum temperatures are 31.5, 27.7 and 24.2°C, respectively, according to the multiannual average for the period of 2001–2007; winds range between 2.57 and 5.14 m·s<sup>-1</sup> in the dry season, in the wet season – between 1.03 and 2.57 m·s<sup>-1</sup>, and in transition season – between

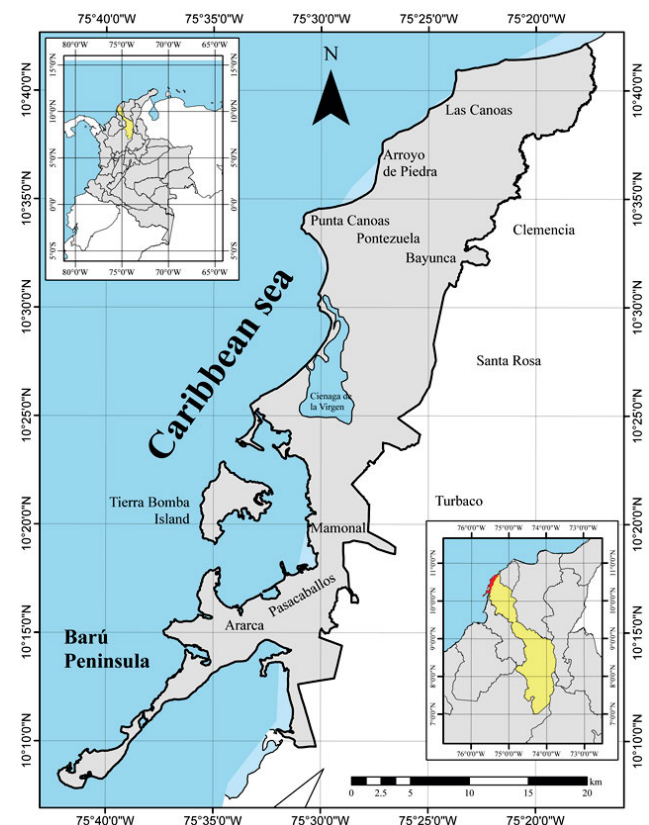


Fig. 1. Cartagena de Indias; source: own elaboration

3.08 and 5.14 m·s<sup>-1</sup>. During the wet season, from April to November, rainfall ranges from 29 to 244 mm·mo<sup>-1</sup>, with the highest rates of rainfall occurring in October [CIOH 2011].

Table 1 compares the pluviometric network used, place and relief for different studies carried out. The majority are observed to have a station density of around 100 km<sup>2</sup>, and it is due to the mountainous area in which they are located to comply with the WMO recommendations (1 station per 250 km<sup>2</sup>), which are generally taken as a reference to verify the network of equipment, despite this, it is difficult to comply with these requirements in a large study area.

### ANALYSIS OF EQUIPMENT AND TECHNIQUES

Applying the WMO [2008] recommended minimum station density for urban areas, a network of nine rain gauges, made up of equipment from different entities distributed over the territory and neighbouring areas at distances between 0.9 and 27 km was used, as shown in Figure 2. Six pieces of equipment belonging to the University of Cartagena (Sp.: Universidad de Cartagena – UDC): UDC (G1) installed 1.5 m above the ground and six months of data recording (Jul–Dec), Turbaco (G2) at 2.0 m above the ground and four months of data recording (Sep–Dec), Technological University of Bolivar (Sp.: Universidad Tecnológica de Bolivar – UTB) (G3) at 2.0 m above the ground and three months of data recording (Oct–Dec), Tierra Bomba (G4) installed 2.0 m off the ground and four months of data recording (Sep–Dec), Mamonal (G5) at 1.5 m above the ground and three months of data recording (Oct–Dec) and Vivarium (G6) at 4.0 m above the ground and four months of data recording (Sep–Dec), are tipping bucket type, of reference HOBO RG3-M (0.2 mm per tip) and installed according to WMO [2008] and Onset [2010] recommendations, as shown in Figure 2. One piece of equipment belonging to General Maritime and Port Directorate (Sp.: Dirección General Marítima

y Portuaria – DIMAR): Oceanographic and Hydrographic Research Center (Sp.: Centro de Investigaciones Oceanográficas e Hidrográficas – CIOH) (G7) installed 1.5 m above the ground and a year of data recording, two pieces of equipment belonging to Institute of Hydrology, Meteorology and Environmental Studies (Sp.: Instituto de Hidrología, Meteorología y Estudios Ambientales – IDEAM): National Open and Distance University (Sp.: Universidad Nacional Abierta y a Distancia – UNAD) (G8) with a year of data recording and equipment of Rafael Núñez International Airport (Sp.: Aeropuerto Rafael Núñez) (G9) and eleven years of data recording, were also used. The last month of recording for nine rain gauges is December 2019 and the minimum time aggregation is 10 min. The input data for analysis depend on the temporal aggregation, for 10 min, these are between 56 for the case of G5 and 1767 for G7. The distribution of the indicated points is due to their topographic representation, considering those already existing and established by other entities, it was not homogeneous to be able to evaluate the largest number of cases.

This study uses a methodology similar to those used by TOKAY *et al.* [2014], TOKAY and ÖZTÜRK [2012], where they use a three-parameter stretched exponential model to determine the inter-gauge correlations. The objective is to find a function to describe the spatial variability between the Pearson’s correlation coefficient *r* and rain gauge distance *d*. This model has been widely used by TESSEMA *et al.* [2020], SUNGMIN and FOELSCHKE [2019], MASCARO [2017], TOKAY *et al.* [2017], DE VOS *et al.* [2017], JAMESON [2017], HYUN *et al.* [2016], SUNILKUMAR *et al.* [2016], TOKAY *et al.* [2016], SHASTRI *et al.* [2015], SVOBODA *et al.* [2015], PELEG *et al.* [2013], MANDAPAKA and QIN [2013], HA *et al.* [2007] to investigate the spatial variability of rainfall. The methodology is complemented with that used by ALFONSO and SCHNABEL [2017], by the characterisation and analysis of rainfall. These methodologies were also selected by analysing the spatial variability of

**Table 1.** Comparison of study area characteristics and network equipment composition for different researches

Study place	Coastal zone	Geographical location		Relief	Area (km <sup>2</sup> )	Recording point	Area per recording point (km <sup>2</sup> )	Reference
		latitude	longitude					
Erbil, Iraq	no	36° N	44° E	mountainous	330.0	9	110.0	KARIM <i>et al.</i> [2018]
Northeastern Algeria	yes	35° N	6° E	mountainous	82,372.0	22	3,744.0	MERNIZ <i>et al.</i> [2019]
Arizona, USA	no	33° N	112° W	mountainous	29,600.0	240	123.0	MASCARO [2018]
Eastern Mediterranean, Israel and Palestine	yes	31° N	35° E	mountainous	15,500.0	3	5,167.0	ORIANI <i>et al.</i> [2017]
Zacatecas, Mexico	no	22° N	102° W	mountainous	75,284.0	760	99.0	RODRIGUEZ GONZÁLEZ <i>et al.</i> [2018]
Cundinamarca, Colombia	no	5° N	74° W	high mountain	18,615.0	182	102.0	GARRIDO-ARÉVALO <i>et al.</i> [2020]
Thur basin, Switzerland	no	47° N	9° E	mountainous	1,700.0	21	81.0	GIRONS LOPEZ <i>et al.</i> [2015]
Kohkiloyeh-Bouyerahmad and Khouzestan provinces, Iran	yes	31° N	50° E	flat	25,000.0	34	735.0	SHAGHAGHIAN and ABEDINI [2013]

Source: own elaboration based on researches from different countries.

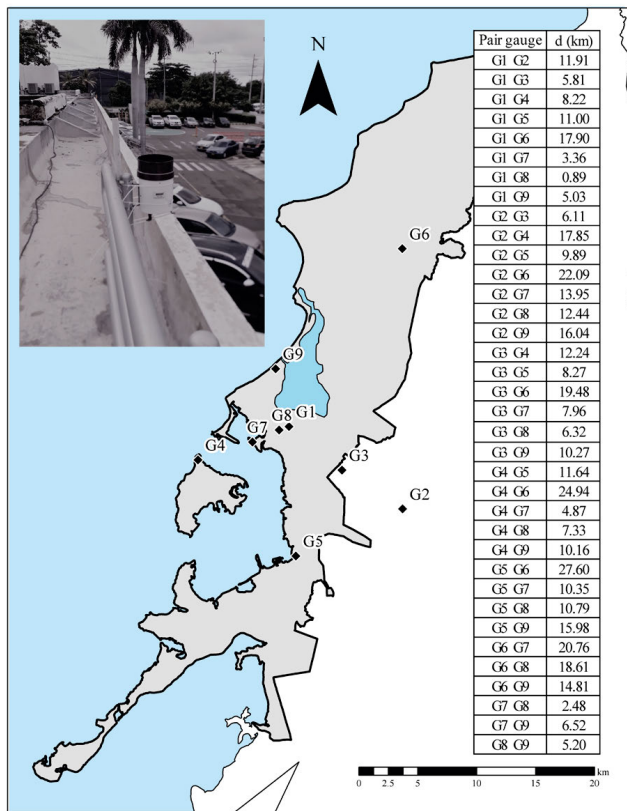


Fig. 2. Network of rain gauges and rain gauge installed in Mamonal (G5);  $d$  = distance between the two gauge sites; source: own elaboration

rainfall in and near the coastal zone, as well as conditions that resemble the needs and location of this study.

The characterisation of the precipitations was carried out using the historical series of data from the G9 station, on an annual and monthly scale, using the total and average data, respectively. On a daily scale, it was carried out by means of frequencies of the average number of days with rain, classified by month and the amount of daily precipitation. The relative frequency corresponds to the quotient between the absolute frequency of certain data and the total data [ALFONSO, SCHNABEL 2017].

The spatial variation of rainfall was studied by comparing precipitation data from different rain gauges for 2019, its standard deviation and coefficient of variation were also calculated in monthly periods. Average ranges per month and standard deviation were calculated for the daily periods. To analyse the intensities, spatial distribution maps of maximum intensities during 10 min for the months of October and November were drawn using the Ordinary Kriging (OK) interpolation method. The average intensity during 10 min and daily precipitation were also related, and boxplots were used to group the data into four groups as a function of precipitation between 0.1 and [0.1–5 mm), [5–10 mm), [10–30 mm), and  $\geq 30$  mm. An important rain event (rainfall event of October 30, 2019) was also analysed where most of the equipment recorded information using rainfall mass curves (cumulative rainfall curve), graphically representing the behaviour of the rainfall [ALFONSO, SCHNABEL 2017].

For the spatial correlation analysis, the relative frequency of duration of rain events was obtained for each station, considering the characteristics that define a rain event [LOZANO-RIVAS 2018].

Then, Pearson's correlation coefficient was applied to 36 pairs of gauge records for 8 different rain accumulation periods ranging from 10 min to 12 h. Rain/no-rain thresholds were considered to exceed a trip (0.2 mm), and were based on 30 min rain accumulation period. A three-parameter exponential function was then applied to the correlation  $r$  and distance  $d$  pairs for each integration period and expressed as in Equation (1):

$$r = r_0 \exp \left[ - \left( \frac{d}{d_0} \right)^s \right] \quad (1)$$

where:  $r_0$  = nugget parameter,  $d$  = distance between the two gauge sites,  $d_0$  = correlation distance,  $s$  = shape parameter.

Despite not having a dual- or triple-tipping-bucket rain gauge network, a correlation of 0.95 was used for a distance  $d = 0$ , according to the results obtained by TOKAY *et al.* [2014].

Finally, a relationship was established between the density of equipment necessary for a network of rain gauges in the urban area of Cartagena de Indias based on the WMO recommendations, the correlation of data and the distance between pieces of equipment, assuming that the afferent area per rain gauge is circular.

The information used from the stations installed by the University of Cartagena can be found on the website of the Environmental Modeling Research Group (GIMA for its acronym in Spanish) [<https://www.gimaunicartagena.org/>]. On the other hand, the information of the Rafael Núñez International Airport and UNAD stations can be requested on the IDEAM website [<http://www.ideam.gov.co/>], and the CIOH station can be requested directly on DIMAR website [<https://www.dimar.mil.co/>].

## RESULTS AND DISCUSSION

### CHARACTERISATION OF RAINFALL IN CARTAGENA DE INDIAS

#### Annual and monthly rainfall

Although the average annual precipitation of the 2009 to 2019 series is 1052 mm, as shown in Figure 3a, the rainiest years were 2010 with 2469 mm and 2011 with 2130.2 mm, and the least rainy year was 2015 with 376 mm, followed by 2019 with 501 mm. The variability in the different hydrological years is notable due to the phenomena associated with the El Niño-Southern Oscillation (ENSO), there are periods with high rainfall followed by low one (2011 to 2012, for example) and vice versa (2009 to 2010, for example), in turn, series of years that behave in a similar way are presented, such as 2012–2015 with a mean of 711 mm, a standard deviation of 268 mm and a coefficient of variation of 38%. For the time series from 2016 to 2019, a mean of 868 mm, a standard deviation of 324 mm, and a coefficient of variation of 37% were obtained. For these time series, the coefficients of variation were very similar. For the time series from 2009 to 2019, a standard deviation of 667.4 mm, and a coefficient of variation of 63% were obtained, indicating high data variation.

Figure 3b represents the average monthly rainfall of the studied series, where it is observed that the hydrological year opens in the month of April (or March in 45% of cases) and the maximum amount of rainfall occurs in the quarter between September and November, where 55% of the annual average rainfall is concentrated, with October being the wettest month of the whole year with 259 mm (25% of the annual average rainfall).

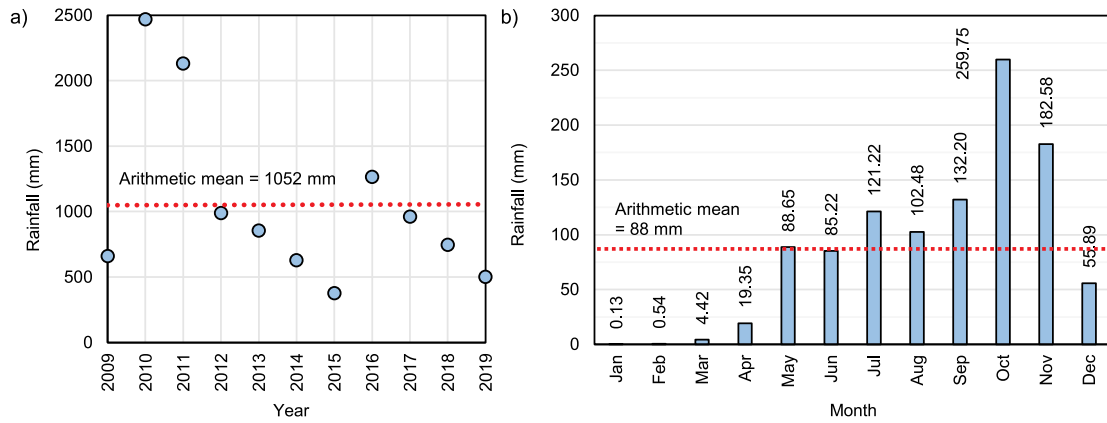


Fig. 3. Average rainfall in Cartagena de Indias for eleven years between 2009 and 2019; a) annual, b) monthly; source: own study

Table 2. Average annual and monthly distribution of daily precipitation frequencies between 2009 and 2019

Month	[0.1–1)	[1–10)	[10–30)	[30–50)	≥50	Month	R-Fre (%)
	mm						
January	1	0	0	0	0	1	1
February	1	1	0	0	0	2	1
March	1	1	1	0	0	3	2
April	3	2	1	1	0	7	5
May	4	4	2	1	1	12	9
June	5	6	3	1	1	16	12
July	4	6	2	1	1	14	10
August	4	7	2	1	1	15	11
September	6	7	3	2	1	19	14
October	6	7	4	2	2	21	16
November	6	5	3	2	1	17	13
December	2	3	1	1	1	8	6
Year	43	49	22	12	9	135	100
R-Fre (%)	32	36	16	9	7	100	

Explanations: R-Fre = relative frequency.  
Source: own study.

October was the month with the highest standard deviation of 176.9 mm and a coefficient of variation of 68%, the third lowest after August and May with coefficients of variation of 53% and 64%, respectively. On the other hand, January has the lowest standard deviation of 0.4 mm, however, its coefficient of variation is 307%, the second highest after February with 332%, which is clear from the months without rain in the data series.

Daily rainfall

Table 2 presents the rainfall frequencies as a function of the average number of days in the annual series of the assigned intervals, it shows that on average 32% of the days of the year represent a rain event less than or equal to 1 mm, 68% of the rains are less than 10 mm, and 43% of the days with rain make up 55% of the average annual rainfall. On the other hand, the difference between months of minimum and maximum rainfall is clearly observed, in addition to the gradual transition between the months of the first half of the year. In March, for example, rains of up to 30 mm begin to occur, a figure which is surpassed in

April and then in May, this gradual transition occurs inversely at the turn of the year (December–January). The rainiest quarter of the year has the greatest amount of rainy days, despite this, most days correspond to less than 10 mm of rainfall, so only 1 or 2 days correspond to more than 50 mm of rainfall, that is, the total amount of the rainiest months are distributed over a few days.

SPATIAL VARIABILITY OF RAINFALL

Spatial variability of rainfall intensities

For the spatial variation of intensities, interpolated maps were made by the Ordinary Kriging (OK) method using the maximum intensities during 10 min for two rainy months (Oct–Nov). As for the month of October, in Figure 4a, it is observed that the maximum intensities are concentrated in the west and centre of the urban area and in the north of the territory, on the contrary, the minimums are presented in the east and the south of the territory. Conversely, for the month of November, Figure 4b shows the maximum intensities in the central zone of Tierra

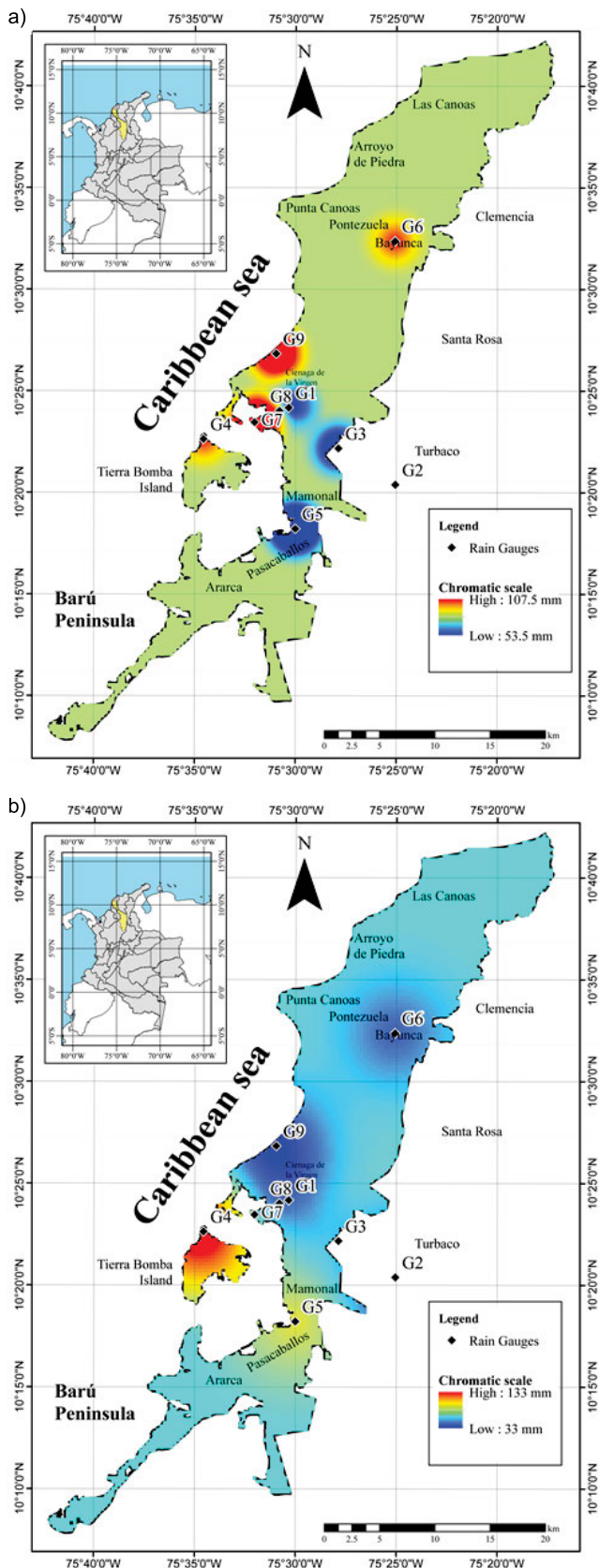


Fig. 4. Maps of maximum intensities during 10 min ( $\text{mm}\cdot\text{h}^{-1}$ ) in the rainiest months: a) October, b) November; source: own study

Bomba Island, and the minimum in the central urban area, in the east and north. This indicates that the maximum intensities are not only variable in space but also in time, and can be synthesised

in the central urban area and the island of Tierra Bomba, which is very close, in contrast to the minima that occur in the east and south of the territory.

The intensity analysis includes the average ratio of the stations between the daily rainfall and the maximum intensities during 10 min, as shown in Figure 5, where it is observed that for the same daily rainfall there may be several maximum intensities, in addition, there is a directly proportional relationship between both variables. Four groups of daily quantities were established, which are presented in Figure 6, between 0.1 and 5 mm ( $N = 229$ ), between 5 and 10 mm ( $N = 30$ ), between 10 and 30 mm ( $N = 20$ ), greater than 30 mm ( $N = 4$ ), the analysis is carried out considering the soil impermeability, mainly in the urban area, therefore, everything that falls will be reflected in the runoff. The difference is not so significant in the first two groups, which are quite similar, but it is between these two and the third (10–30 mm) and fourth ( $>30$  mm) groups.

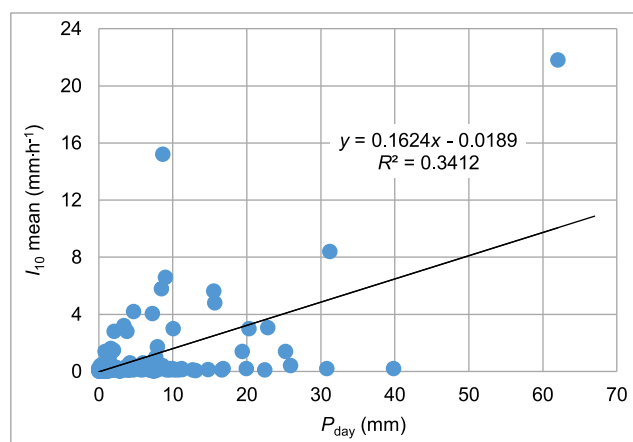


Fig. 5. Relationship between average rainfall daily ( $P_{\text{day}}$ ) and intensity during 10 min ( $I_{10}$ ) with the line of best fit linear regression ( $N = 290$ ); source: own study

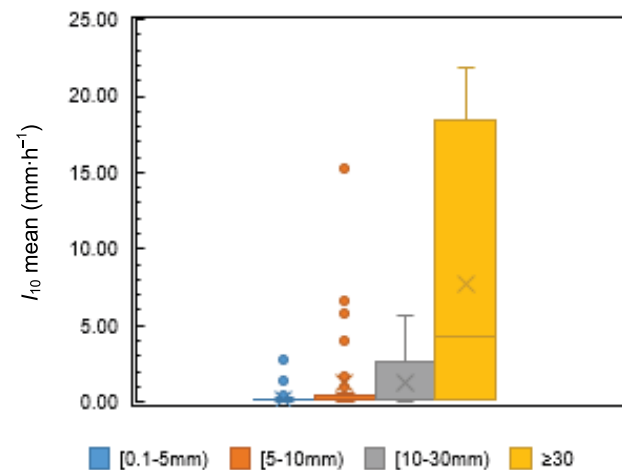


Fig. 6. Grouped intensity during 10 min ( $I_{10}$ ); source: own study

### Analysis of rainfall event

Figure 7 represents the mass curve resulting from accumulated data from the rainfall event of October 30, 2019, which began at 12:30 detected by G6 in the north, and then distributed towards

the south, where most of the rain gauges recorded information, except for G7 and G9. In G6 it lasted 30 min with a constant intensity and then gradually decreased. One hour after it started, in the urban area, it was detected by stations G1 and G3 with intensities a little lower than G6, 10 min later by G8, G2 and G5 in the urban area, to the east and south respectively, and finally 30 minutes later in Tierra Bomba Island by G4.

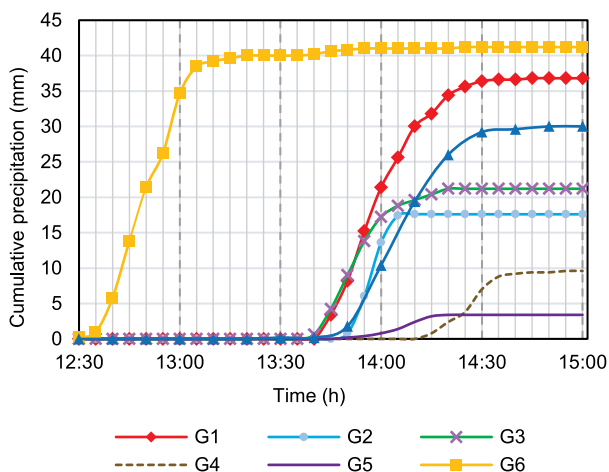


Fig. 7. Precipitation mass curve of the rain event of October 30, 2019; source: own study

It is evident that the rain predominated in the southwest direction, so the maximum quantities and intensities were presented at the stations located in that direction, when, for example, comparing G1 and G3, although they began to register at the same time and even had the same intensity for about 15 min, G1, which is further east, registered almost twice as much precipitation as G3. In turn, G3 registered more rainfall than G2, which is further east. On the other hand, G5 and G4, in that order were the last stations to record information, G4, located to the west, had higher intensities and obtained almost three times the precipitation of G5 located to the south.

Figure 8 shows the percentage of the duration of rain events for each of the stations, it can be seen that in the city and

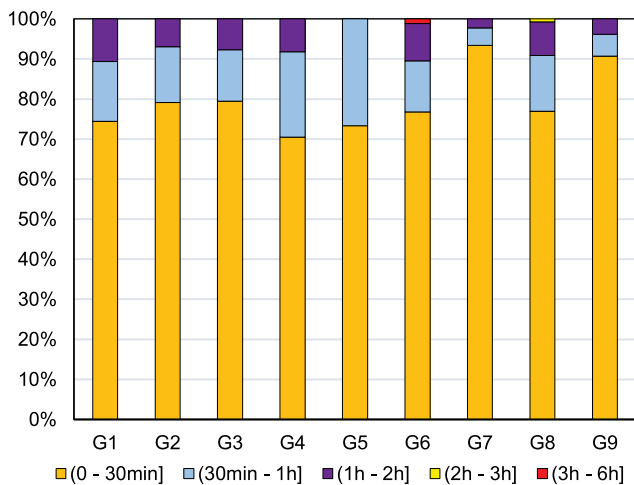


Fig. 8. Percentage of rain events duration for each gauge; source: own study

surrounding areas 70% of the rain events have a duration of less than 30 min, and 90% less than 1 h. The distribution of rain durations for nearby stations is very similar, for example, at central stations G8 and G1 (0.89 km), and the eastern G2 and G3 (6.11 km), as for station G5, 100% of the rain events are less than 1 h in duration, station G6 was the only one to record an event lasting between 3 and 6 h.

### SPATIAL CORRELATION

With the exponential function of three parameters, it was found that for the observation period in rainfall integrations of 30 min, the correlations were less than 0.8, 0.5, and 0.2 at distances of 1, 3 and 7 km, respectively, as shown in Figure 9. The nugget parameter calculated for the analysed stations was 0.89. The distance correlation and the shape parameter were 4.42 km and 1.01, respectively, for the exponential fit. The root mean square error (RMSE), which shows the goodness of fit, was 0.09.

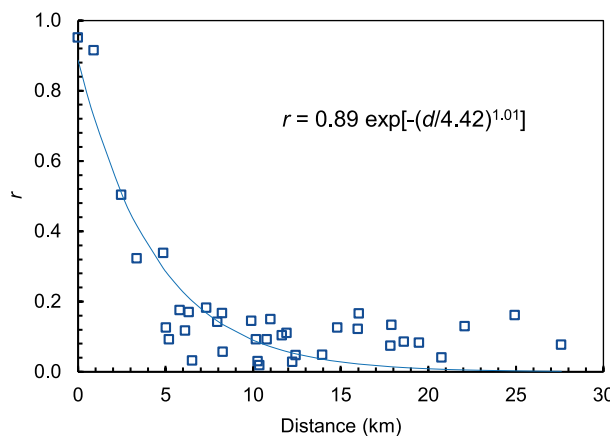


Fig. 9. Intergauge correlations (squares) and the fitted exponential function (curve) for 30-min time averaging;  $r$  = correlation coefficient,  $RMSE$  = root mean square error,  $d$  = distance between the two gauge sites; source: own study

Table 3 summarises information on location, surface and results obtained in different studies, including this one, where a three-parameter exponential function was used to analyse the spatial variability of rainfall. When comparing them with each other, it is found that the places closest to the Equator line present higher variabilities, which can be justified mainly by the difference in latitudes of the study areas, where atmospheric phenomena allow the distribution of rainfall to be more heterogeneous.

When comparing, for example, our results with those obtained by TOKAY *et al.* [2014], who got  $r_0 = 0.93$ ,  $d_0 = 12.2$  and  $s = 0.57$ , it is concluded that on the Delmarva Peninsula the rain gauges location can be more widely spaced than in Cartagena de Indias. For example, to obtain a correlation of 0.5 in both places, the equipment on the Delmarva Peninsula can be located three times the distance obtained in Cartagena de Indias, meaning that the spatial variability of the rainfall in the latter is higher, and this was expected due to the difference in latitudes. On the other hand, if we compare our results with those obtained by MANDAPAKA and QIN [2013] in Singapore, whose study area is almost on the equatorial line and who obtained  $r_0 = 1$ ,  $d_0 = 10.1$  and  $s = 0.62$ , the spacing between gauges, even though it is a little higher, is more

**Table 3.** Summary of results obtained in research that used a three-parameter exponential function

Study place	Coastal zone	Geographical location		Area (km <sup>2</sup> )	Recording points	Distance (km) for each correlation			Parameter			Reference
		latitude	longitude			0.8	0.6	0.4	$r_0$	$d_0$	$s$	
Amsterdam, the Netherlands	no	52.3°N	4.8°E	575.0	63	–	–	28.00	0.58	130.00	0.65	De Vos <i>et al.</i> [2017]
Hradec Králové Region, Czech Republic	no	50°N	16°E	4,759.0	38	2.80	34.00	199.00	1.00	260.00	0.33	SVOBODA <i>et al.</i> [2015]
Feldbach, Austria	no	47°N	16°E	300.0	150	4.00	11.40	22.30	0.95	26.00	0.94	SUNGMIN and FOELSCHKE [2019]
Delmarva Peninsula, USA	yes	39°N	75°W	14,127.0	11	0.62	4.00	12.80	0.93	17.20	0.57	TOKAY <i>et al.</i> [2014]
Kentucky, USA	no	38° N	85° W	1,022.0	17	2.80	9.30	21.30	1.00	24.19	0.70	HYUN <i>et al.</i> [2016]
Virginia, USA	no	37.9°N	75.4°W	4.3	6	0.88	4.20	12.30	0.99	14.70	0.55	TOKAY <i>et al.</i> [2016]
Oklahoma, USA	no	36.78°N	97.18°W	80.0	13	3.60	6.40	9.50	1.00	10.10	1.49	TOKAY <i>et al.</i> [2017]
Korean peninsula	yes	36°N	127°E	100,210.0	464	10.49	24.00	43.00	1.00	47.00	1.00	HA <i>et al.</i> [2007]
Central Arizona, USA	no	33°N	112°W	29,600.0	310	0.80	3.30	9.20	1.00	10.70	0.57	MASCARO [2017]
Gal'ed, Israel	no	32°N	35°E	4.0	14	2.50	5.10	8.30	0.99	9.00	1.20	PELEG <i>et al.</i> [2013]
Gadanki, India	no	13°N	79°E	2,500.0	36	0	10.60	20.50	0.80	27.06	1.33	SUNILKUMAR <i>et al.</i> [2016]
Cartagena, Colombia	yes	10°N	75°W	80.0	9	0.48	1.76	3.54	0.89	4.42	1.01	own study
Upper Gana watershed, Ethiopia	no	7.58°N	37.75°E	16.9	11	1.00	6.40	21.20	0.95	27.89	0.53	TESSEMA <i>et al.</i> [2020]
Singapore	yes	1.2°N	103°E	710.0	49	0.90	3.40	8.80	1.00	10.10	0.62	MANDAPAKA and QIN [2013]

Explanations:  $r_0$  = nugget parameter,  $d_0$  = correlation distance,  $s$  = shape parameter.  
 Source: own elaboration based on researches from different countries.

similar. In this way, the places that are between the latitudes 10° N and 10° S present higher variabilities.

It is also noted that in coastal areas the spatial variability of rain is much higher, although this is well known, in Table 3 it is evident and verified, thus in the Upper Gana watershed (Ethiopia) or in Gadanki (India), gauges may be more spaced than in Cartagena or Singapore, although they are all between the equatorial line and 10° N and 10° S.

Another aspect to highlight is the effect of longitude, since the places to the west present higher variabilities and are justified by global phenomena such as ENSO. Thus, when comparing longitudes of different points with similar latitudes, the variability is much greater in such places as Kentucky, Virginia or Oklahoma (USA) than on the Korean peninsula, despite the fact that the latter is located in a coastal area. Other examples are central Arizona (USA) and Gal'ed (Israel) in the east, while the variability is greater in Cartagena (Colombia) than

in Gadanki (India), the Upper Gana watershed (Ethiopia) or Singapore despite the fact that the latitude of the latter is much smaller.

### EXPONENTIAL ADJUSTMENT PARAMETERS

The nugget parameter was higher than 0.88 for the different groups considered, Figure 10a, increasing with long periods of grouping, finding minimum and maximum values of 0.89 and 0.98 for 30 min and 6 h, respectively, this shows that the variability between stations is quite pronounced for short periods of rain. The correlation distance was usually between 4.3 and 5.3 km, but it was as low as 2.2 km and as high as 7 km for 10 min and 12 h of grouping, respectively, Figure 10b. The shape parameter remained constant at around 1, except for the 20 min grouping which was almost 5 (Fig. 10c). The RMSE was less than 0.1 for 30 min but increased to 0.19 in 12 h of grouping (Fig. 10d).

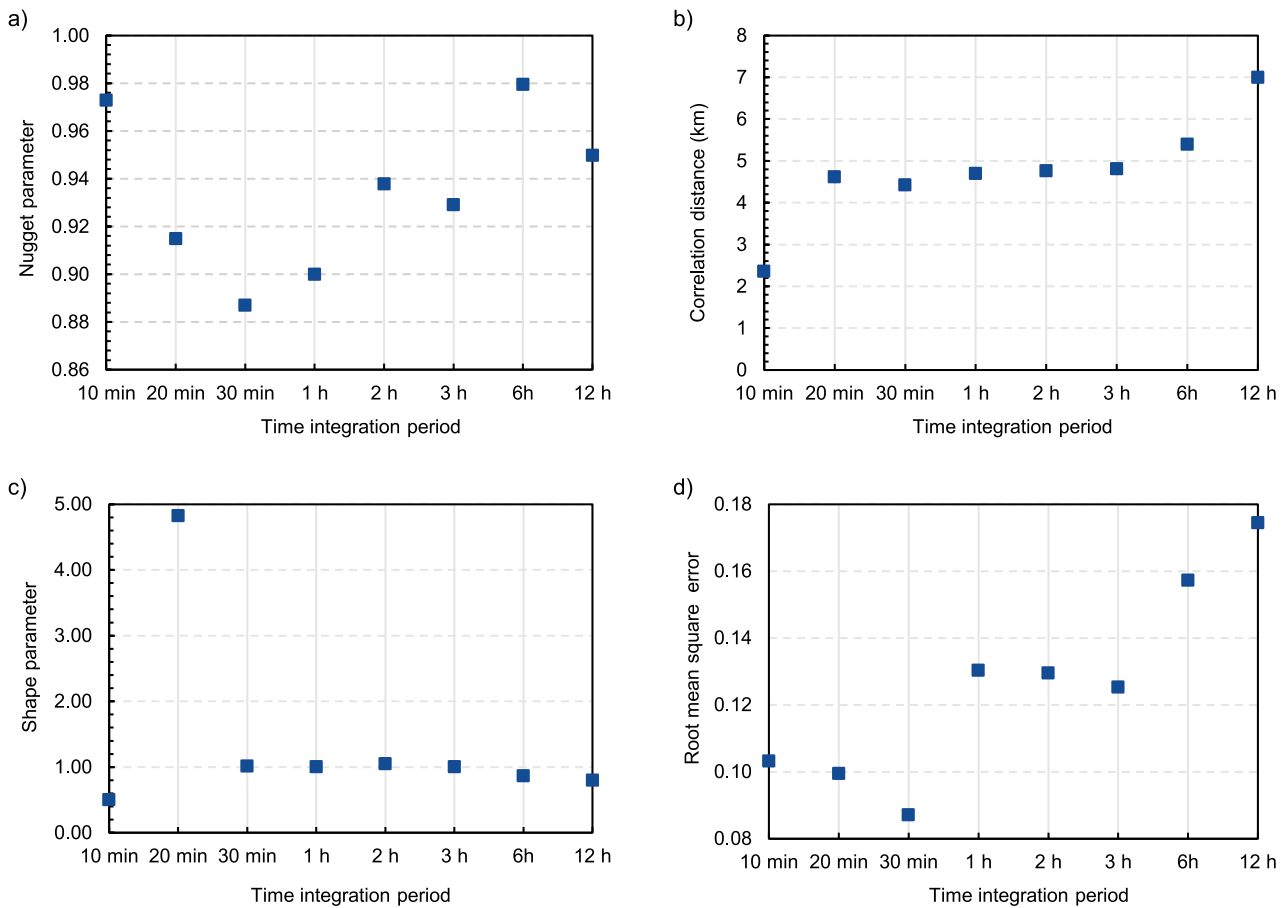


**Fig. 10.** Dependence of: a) nugget parameter, b) correlation distance, c) shape parameter of the exponential function, d) root mean square error (RMSE), on the averaging time scale ranging from 10 min to 12 h; source: own study

For the nugget parameter, TOKAY *et al.* [2014] had results greater than 0.88, similar to those in the present study, the maximum deviation was 7.7% and was presented in groups of 10 min. The correlation distance had higher values, ranging between 10 and 180 approximately. The shape parameter had values between 0.52 and 0.67. The values for RMSE were less than 0.09.

### RAIN GAUGE NETWORK IN THE URBAN AREA

A hydrological station has a significant afferent area that, according to the recommendation of the World Meteorological Organization (WMO), obeys the socio-economic and physical-climatic conditions, the area per rainfall station must be between 10 and 20 km<sup>2</sup> in urban areas [WMO 2008]. Assuming that the contributing area of a rain gauge is distributed in a circular way with the equipment as the centre and the afferent circumferences of each rain gauge cut tangentially, as in Figure 11, relationships can be established concerning the distance between the two gauge sites ( $d$ ), the correlation ( $r$ ) and the number of gauges ( $N$ ), knowing that the urban area is approximately 100 km<sup>2</sup>. Figure 12, which includes the limits of the areas recommended by the WMO, 3.6 and 5 km for 10 and 20 km<sup>2</sup>, respectively, notes that both the  $d-r$  and  $d-N$  relationships are inversely proportional. In this way, in the urban area of Cartagena de Indias, 10 stations would be necessary to record rainfall information at a distance of 3.6 km, to obtain a correlation of 0.6, and at least 6 rain gauges

per 5 km to get a correlation of 0.5. The location of the station in the built-up area must also meet the requirements of the WMO regarding the distances from objects that may affect the measurement result (trees, buildings, etc.). Although the correlation was calculated with the adjustment equation for rains with durations of 30 min, it was compared with other rain durations and the results were higher than 4% in most cases, except for rains with durations of 10 min, which were lower by 30%. Although it is not depicted in Figures 11 and 12, it can be projected that for an installed rain gauge, at a distance ( $R$ ) greater than 6.5 km (that is,  $d > 13$  km), the data correlation ( $r$ ) is less than 0.2.

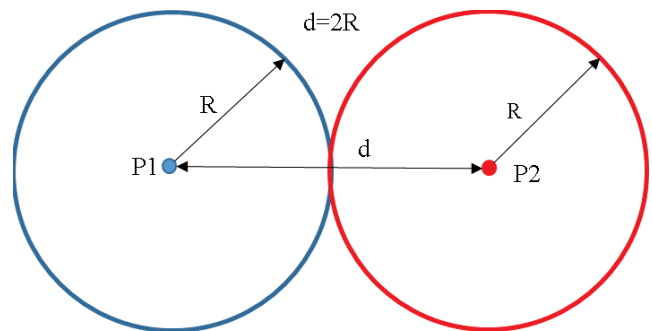


**Fig. 11.** Contributing area distribution between rain gauges;  $d$  = distance between the two gauge sites,  $R$  = circumference radius of each rain gauge; source: own study

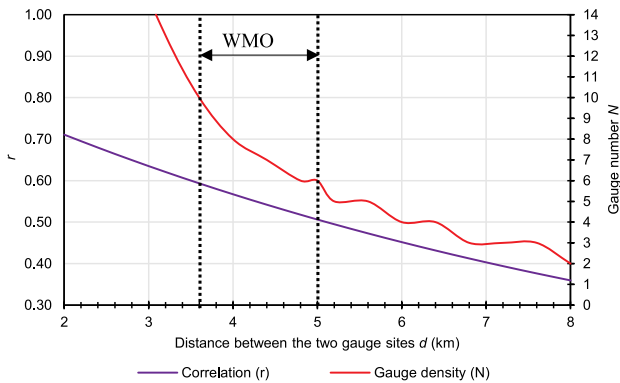


Fig. 12. Gauge density and correlation vs. gauge distance; source: own study

## CONCLUSIONS

The average annual rainfall recorded by the Rafael Núñez International Airport station is 1052 mm. The annual amount of precipitation is quite uneven, 2010 stands out with the highest rainfall of 2469 mm and 2015 – as the least rainy with 376 mm, this variability is a typical phenomenon associated with El Niño-Southern Oscillation (ENSO). The average total annual rainfall is concentrated in the rainiest quarter, comprised of September, October and November, which consists of 43% of days with rain, that makes up 55% of the total precipitation. The wettest month is October with an annual average rainfall of 25% and the highest number of days with rain, 16% of the total daily precipitation frequencies.

The data recorded in one year provided the information for the investigation of the spatial variability of rainfall. Both the monthly standard deviations and the highest and lowest daily average ranges, recorded in 2019, were presented in the rainiest (October) and least rainy (December) months, respectively. Geographically, the highest rainfall occurred at the stations in the north, west and in the urban (central) area of the territory, while the lowest was in the east and south. This is mainly justified by the location of the city and the prevailing winds from the N (towards the south) and NE (towards the southwest). Regarding the intensities, it was maximum in the urban area and on Tierra Bomba Island, and minimum in the east and south, adding that the days with higher rainfall showed the greatest variations.

It is important to note that 70% of the rain events had a duration of less than 30 min, and 90% less than 1 h, so only 10% or less had a duration greater than 1 h.

The spatial variability was more pronounced at short distances as well as correlations below 0.8 at distances of 1 km for the experimental period in 30 min of integration. The correlation gradually decreased from 0.5 to 0.2 between 3 and 7 km and was less than 0.1 for distances greater than 10 km. The three exponential function parameters had good adjustments in all evaluated cases, with differences between the observed and adjusted values being quite small. The root mean square (RMSE) had a maximum value of 0.17 and a minimum of 0.09, for the aggregations of 12 h and 30 min, respectively.

The nugget parameter, which is the correlation of the installed rain gauges, was greater than 0.88. The shape

parameter had, in most cases, values around 1, and the correlation distance was between 4.3 and 5.3 km.

In the urban area of Cartagena de Indias, it would be necessary for 10 stations that record rainfall information located at 3.6 km to obtain a correlation of 0.6, and at least 6 to 5 km to obtain a correlation of 0.5, to meet the minimum and maximum range of rainfall density recommended by the WMO, respectively.

Due to the importance of the city and the issues of rainfall, distribution and spatial variability of rainfall, in addition to its versatility in different fields of action, it is recommended to continue researching, mainly with a wider network of rain gauges, with a dual- or triple-tipping-bucket rain gauge networks, and with a larger annual series of data. Likewise, it is not limited only to the urban and surrounding area, but also covers a wider area where quite important economic and engineering activities are carried out. In turn, it would be important to assess the status of the considered equipment network and optimise it by relocating or expanding equipment.

## ACKNOWLEDGEMENTS

The work presented in this paper has been supported by the University of Cartagena as a result of the research project “Estudio de la variabilidad espacial de la lluvia en la ciudad de Cartagena de Indias” carried out by the Environmental Modeling Research Group (GIMA for its acronym in Spanish). We are grateful to the Universidad de Cartagena, the population of Tierra Bomba Island, the Vivarium de Caribe Foundation, YARA Colombia SAS company and Universidad Tecnológica de Bolívar for allowing us to install and ensure the safety of the rain gauges located in their territory, IDEAM, DIMAR and CIOH for sharing the rain data collected.

## REFERENCES

- ADHIKARY S.K., YILMAZ A.G., MUTTIL N. 2015. Optimal design of rain gauge network in the Middle Yarra River catchment, Australia. *Hydrological Processes*. Vol. 29(11) p. 2582–2599. DOI 10.1002/hyp.10389.
- Alcaldía Mayor de Cartagena de Indias 2001. Plan de Ordenamiento Territorial del Distrito Turístico y Cultural de Cartagena de Indias [Territorial Planning Plan of the Tourist and Cultural District of Cartagena de Indias]. [online]. Cartagena de Indias. [Access 30.05.2019]. Available at: [https://vuc.cartagena.gov.co/documentos/normatividad/DECRETO\\_0977\\_de\\_2001.pdf](https://vuc.cartagena.gov.co/documentos/normatividad/DECRETO_0977_de_2001.pdf)
- ALFONSO A., SCHNABEL S. 2017. Variación espacial de las precipitaciones en una pequeña cuenca hidrográfica del suroeste de España [Spatial variation of rainfall in a small hydrographic basin in southwestern Spain]. *Geographicalia*. Vol. 69 p. 65–91. DOI 10.26754/ojs\_geoph/geoph.2017692319.
- CIOH 2011. Climatología de los principales puertos del Caribe colombiano: Cartagena de Indias [Climatology of the main ports of the Colombian Caribbean: Cartagena de Indias]. [online]. D.T. y C. Cartagena de Indias. Centro de Investigaciones Oceanográficas e Hidrográficas. [Access 26.03.2019]. Available at: <https://www.cioh.org.co/meteorologia/ResumenCartagena.php>
- CORTÉS A.C. 2010. Análisis de la variabilidad espacial y temporal de la precipitación en una ciudad de media montaña Andina caso de estudio: Manizales [Analysis of the spatial and temporal

- variability of precipitation in an Andean mid-mountain city case study: Manizales] [online]. Universidad Nacional de Colombia Sede Manizales. [Access 17.04.2019]. Available at: <https://repositorio.unal.edu.co/handle/unal/7246>
- DE VOS L., LEIJNSE H., OVEREEM A., UIJLENHOET R. 2017. The potential of urban rainfall monitoring with crowdsourced automatic weather stations in Amsterdam. *Hydrology and Earth System Sciences*. Vol. 21(2) p. 765–777. DOI 10.5194/hess-21-765-2017.
- DEY P., MUJUMDAR P.P. 2019. On the uniformity of rainfall distribution over India. *Journal of Hydrology*. Vol. 578, 124017. DOI 10.1016/j.jhydrol.2019.124017.
- EPA Cartagena. 2019. Ordenamiento Territorial [Territorial Ordering]. [online]. Establecimiento Público Ambiental Cartagena. [Access 05.04.2020]. Available at: <http://observatorio.epacartagena.gov.co/gestion-ambiental/generalidades-de-cartagena/territorio/ordenamiento-territorial/>
- GARCÍA F., CRUZ I. 2009. Variabilidad de la precipitación pluvial en la región Pacífico Norte de México [Variability of rainfall in the north pacific region of México]. *Agrociencia*. Vol. 43(1) p. 1–9.
- GARRIDO-ARÉVALO A.R., AGUDELO-OTÁLORA L.M., OBREGÓN-NEIRA N., GARRIDO-ARÉVALO V., QUIÑONES-BOLAÑOS E.E., NARAEI P., MEHRVAR M., BUSTILLO-LECOMPTÉ C.F. 2020. Application of artificial neural network and information entropy theory to assess rainfall station distribution: A case study from Colombia. *Water*. Vol. 12 (7) p. 1–18. DOI 10.3390/w12071973.
- GIRONS LOPEZ M., WENNERSTRÖM H., NORDÉN L.Å., SEIBERT J. 2015. Location and density of rain gauges for the estimation of spatial varying precipitation. *Geografiska Annaler, Series A: Physical Geography*. Vol. 97(1) p. 167–179. DOI 10.3390/w12071973.
- GYASI-AGYEI Y. 2020. Identification of the optimum rain gauge network density for hydrological modelling based on radar rainfall analysis. *Water*. Vol. 12(7), 1906. DOI 10.3390/w12071906.
- HA K.J., JEON E.H., OH H.M. 2007. Spatial and temporal characteristics of precipitation using an extensive network of ground gauge in the Korean Peninsula. *Atmospheric Research*. Vol. 86(3–4) p. 330–339. DOI 10.1016/j.atmosres.2007.07.002.
- HYUN J.-Y., ROCKAWAY T.D., FRENCH M.N. 2016. Ground-level rainfall variation in Jefferson County, Kentucky. *Journal of Hydrologic Engineering*. Vol. 21(12), 05016029. DOI 10.1061/(ASCE)HE.1943-5584.0001438.
- INVEMAR, MADRS, Alcaldía Mayor de Cartagena de Indias. 2012. Lineamientos para la adaptación al cambio climático de Cartagena de Indias. Proyecto Integración de la Adaptación al Cambio Climático en la Planificación Territorial y Gestión Sectorial de Cartagena de Indias [Guidelines for adaptation to climate change in Cartagena de Indias. Project Integration of Adaptation to Climate Change in Territorial Planning and Sectoral Management of Cartagena de Indias] [online]. Eds. G.X. Rojas, J. Blanco, F. Navarrete. 55<sup>th</sup> ed. Cartagena, Colombia. Instituto de Investigaciones Marinas y Costeras. [Access 17.04.2019]. Available at: <http://hdl.handle.net/1834/6606>
- INVEMAR, MADRS, Alcaldía Mayor de Cartagena de Indias, CDKN 2014. Integración de la adaptación al cambio climático en la planificación territorial y gestión sectorial de Cartagena de Indias. Informe técnico final [Integration of adaptation to climate change in the territorial planning and sectoral management of Cartagena de Indias. Final technical report]. [online]. Eds. X. Rojas G., M. Ulloque, M. Lacoste. 62<sup>nd</sup> ed. Serie de Publicaciones Generales del Invepar. No. 62. Santa Marta. Instituto de Investigaciones Marinas y Costeras pp. 222 [Access 16.04.2019]. Available at: <http://hdl.handle.net/1834/6663>
- IPCC 1997. The regional impacts of climate change: An assessment of vulnerability. Eds. R. Watson, M. Zinyowera, M. Richard, D. Dokken. UK. Cambridge University Press pp. 530.
- JAMESON A.R. 2017. Spatial and temporal network sampling effects on the correlation and variance structures of rain observations. *Journal of Hydrometeorology*. Vol. 18. No. 1 p. 187–196. DOI 10.1175/JHM-D-16-0129.1.
- KARIM T.H., KEYA D.R., AMIN Z.A. 2018. Temporal and spatial variations in annual rainfall distribution in Erbil province. *Outlook on Agriculture*. Vol. 47(1) p. 59–67. DOI 10.1177/0030727018762968.
- LOZANO-RIVAS W. 2018. Clima, hidrología y meteorología: Para ciencias ambientales e ingeniería [Climate, hydrology, and meteorology: For environmental science and engineering]. Bogotá. Universidad Piloto de Colombia. ISBN 9789588957760 pp. 508.
- MANDAPAKA P.V., QIN X. 2013. Analysis and characterization of probability distribution and small-scale spatial variability of rainfall in Singapore using a dense gauge network. *Journal of Applied Meteorology and Climatology*. Vol. 52(12) p. 2781–2796. DOI 10.1175/JAMC-D-13-0115.1.
- MARKONIS Y., BATELIS S.C., DIMAKOS Y., MOSCHOU E., KOUTSOYIANNIS D. 2017. Temporal and spatial variability of rainfall over Greece. *Theoretical and Applied Climatology*. Vol. 130(1–2) p. 217–232. DOI 10.1007/s00704-016-1878-7.
- MASCARO G. 2017. Multiscale spatial and temporal statistical properties of rainfall in central Arizona. *Journal of Hydrometeorology*. Vol. 18(1) p. 227–245. DOI 10.1175/JHM-D-16-0167.1.
- MASCARO G. 2018. On the distributions of annual and seasonal daily rainfall extremes in central Arizona and their spatial variability. *Journal of Hydrology*. Vol. 559 p. 266–281. DOI 10.1016/j.jhydrol.2018.02.011.
- MERNIZ N., TAHAR A., BENMEHAIA A.M. 2019. Statistical assessment of rainfall variability and trends in northeastern Algeria. *Journal of Water and Land Development*. Vol. 40(1) p. 87–96. DOI 10.2478/jwld-2019-0009.
- MITRA A., APTE A., GOVINDARAJAN R., VASAN V., VADLAMANI S. 2018. Spatio-temporal patterns of daily Indian summer monsoon rainfall. *Dynamics and Statistics of the Climate System*. Vol. 3(1) p. 1–16. DOI 10.1093/climsys/dzy010.
- Onset 2010. Data logging rain gauge (RG3 and RG3-M) user's manual. [online]. Onset. [Access 15.04.2019]. Available at: [https://www.onsetcomp.com/files/manual\\_pdfs/10241-D-MAN-RG3.pdf](https://www.onsetcomp.com/files/manual_pdfs/10241-D-MAN-RG3.pdf)
- ORIANI F., OHANA-LEVI N., MARRA F., STRAUBHAAR J., MARIETHOZ G., RENARD P., MORIN E. 2017. Simulating small-scale rainfall fields conditioned by weather state and elevation: A data-driven approach based on rainfall radar images. *Water Resources Research*. Vol. 53(10) p. 8512–8532. DOI 10.1002/2017WR020876.
- PELEG N., BEN-ASHER M., MORIN E. 2013. Radar subpixel-scale rainfall variability and uncertainty: Lessons learned from observations of a dense rain-gauge network. *Hydrology and Earth System Sciences*. Vol. 17(6) p. 2195–2208. DOI 10.5194/hess-17-2195-2013.
- PRIYAN K. 2015. Spatial and temporal variability of rainfall in Anand district of Gujarat state. *Aquatic Procedia*. Vol. 4 p. 713–720. DOI 10.1016/j.aqpro.2015.02.092.
- RODRÍGUEZ GONZÁLEZ B., PINEDA MARTÍNEZ L.F., GUERRA COBIÁN V.H. 2018. Análisis de la variabilidad de las precipitaciones en el Estado de Zacatecas, México, por medio de información satelital y pluviométrica [Precipitation variability analysis in the State of Zacatecas, México, by utilizing satellite information and gauges]. *Ingeniería Investigación y Tecnología*. Vol. 19(4) p. 1–12. DOI 10.22201/ifi.25940732e.2018.19n4.031.

- SHAGHAGHIAN M.R., ABEDINI M.J. 2013. Rain gauge network design using coupled geostatistical and multivariate techniques. *Scientia Iranica*. Vol. 20(2) p. 259–269. DOI 10.1016/j.scient.2012.11.014.
- SHASTRI H., PAUL S., GHOSH S., KARMAKAR S. 2015. Impacts of urbanization on Indian summer monsoon rainfall extremes. *Journal of Geophysical Research: Atmospheres*. Vol. 120 p. 495–516. DOI 10.1002/2014JD022061.
- SUNGMIN O., FOELSCH U. 2019. Assessment of spatial uncertainty of heavy rainfall at catchment scale using a dense gauge network. *Hydrology and Earth System Sciences*. Vol. 23(7) p. 2863–2875. DOI 10.5194/hess-23-2863-2019.
- SUNILKUMAR K., NARAYANA RAO T., SATHEESHKUMAR S. 2016. Assessment of small-scale variability of rainfall and multi-satellite precipitation estimates using measurements from a dense rain gauge network in Southeast India. *Hydrology and Earth System Sciences*. Vol. 20(5) p. 1719–1735. DOI 10.5194/hess-20-1719-2016.
- SVOBODA V., MÁČA P., HANEL M., PECH P. 2015. Spatial correlation structure of monthly rainfall at a mesoscale region of north-eastern Bohemia. *Theoretical and Applied Climatology*. Vol. 121 (1–2) p. 359–375. DOI 10.1007/s00704-014-1241-9.
- TESSEMA K.B., HAILE A.T., AMENCHO N.W., HABIB E. 2020. Effect of rainfall variability and gauge representativeness on satellite rainfall accuracy in a small upland watershed in southern Ethiopia. *Hydrological Sciences Journal. Spec. Iss. Hydrological data: Opportunities and barriers*. DOI 10.1080/02626667.2020.1770766.
- TOKAY A., D'ADDERIO L.P., PORCÙ F., WOLFF D.B., PETERSEN W.A. 2017. A field study of footprint-scale variability of raindrop size distribution. *Journal of Hydrometeorology*. Vol. 18(12) p. 3165–3179. DOI 10.1175/JHM-D-17-0003.1.
- TOKAY A., D'ADDERIO L.P., WOLFF D.B., PETERSEN W.A. 2016. A field study of pixel-scale variability of raindrop size distribution in the Mid-Atlantic region. *Journal of Hydrometeorology*. Vol. 17(6) p. 1855–1868. DOI 10.1175/JHM-D-15-0159.1.
- TOKAY A., ÖZTÜRK K. 2012. An experimental study of the small-scale variability of rainfall. *Journal of Hydrometeorology*. Vol. 13(1) p. 351–365. DOI 10.1175/JHM-D-11-014.1.
- TOKAY A., ROCHE R.J., BASHOR P.G. 2014. An experimental study of spatial variability of rainfall. *Journal of Hydrometeorology*. Vol. 15(2) p. 801–812. DOI 10.1175/JHM-D-13-031.1.
- WARWADE P., TIWARI S., RANJAN S., CHANDNIHA S.K., ADAMOWSKI J. 2018. Spatio-temporal variation of rainfall over Bihar State, India. *Journal of Water and Land Development*. No. 36 p. 183–197. DOI 10.2478/jwld-2018-0018.
- WMO 2008. Guide to hydrological practices. Vol. I: Hydrology – From measurement to hydrological information No. 168. 6<sup>th</sup> ed. [online]. World Meteorological Organization. [Access 17.04.2019]. Available at: <https://whyco.org/guide/>